Proceedings Paper:
Xie, Y, Zhang, X, Meng, W et al. (4 more authors) (2020) Coupled Sliding Mode Control of an Omnidirectional Mobile Robot with Variable Modes*. In: 2020 IEEE/ASME International Conference on Advanced Intelligent Mechatronics (AIM). 2020 IEEE/ASME International Conference on Advanced Intelligent Mechatronics (AIM 2020), 06-09 Jul 2020, Boston, Massachusetts, USA. IEEE , pp. 1792-1797. ISBN 978-1-7281-6795-4

https://doi.org/10.1109/aim43001.2020.9158823

Coupled Sliding Mode Control of an Omnidirectional Mobile Robot with Variable Modes*

Yuanlong Xie, Xiaolong Zhang, Wei Meng, Shane Xie, Liquan Jiang, Jie Meng, and Shuting Wang

Abstract—Adequate tracking flexibility and accuracy of the omnidirectional mobile robot are difficult to be achieved with one fixed control frame due to the time-varying dynamics. This paper presents a coupled sliding mode control (CSMC) method, which is able to switch the alternative modes to adapt to operational conditions and perform a satisfactory tracking control. The design begins with constructing a unified state error model for the considered multiple modes. Then, by exploiting novel coupled sliding surfaces, a CSMC is formulated which can effectively alleviate the chattering. Meanwhile, based on the desired and current state information, a two-stage fuzzy switching mechanism is proposed to accomplish an autonomous switched tracking control. Theoretical analysis reveals that the system reaches the sliding manifold in finite time, and the convergence of the state errors can be guaranteed. Experiments on a real-life four-wheeled mobile robot validate the effectiveness and superiority of this control method comparing with single-mode control scheme or conventional methods.

I. Introduction

Mobiles robot attract a significant interest among engineers and researchers due to the good dexterity, maneuverability and high-efficiency [1]. Various prototypes and products of mobile robots have been developed as a high integration of robot technologies on perception, navigation and manipulation [2]-[3]. For example, a compound mobile robot, which is composed of a mobile platform with one or more onboard robotic arms mounted on it, allows performing tasks requiring locomotion and manipulation. Among them, the omnidirectional mobile robot (OMR) receives considerate attention profiting from its four independently steering and driving features [4]. This type of robot can be configured in multiple kinematic modes, such as diagonal- move steer mode, Ackerman mode, skid mode and zero-radius steer mode [5]. Comparing with traditional mobile robots with only one single-mode, it has better adaptability and practicability in cluttered spaces or confined environment. However, as the OMR goes further into various applications, the precise chassis tracking control remains a challenging task due to the changing dynamics and system uncertainties.

*Research is supported in part by China Postdoctoral Science Foundation under Grant no. 2019M650179, in part by Hubei technical innovation project under Grant no. 2018AAA027, and in part by Guangdong major science and technology project under Grant no. 2019B090919003. Shuting Wang is the corresponding author (wangst@hust.edu.cn).

Y. Xie, X. Zhang, L. Jiang, J. Meng and S. Wang are with the School of Mechanical Science and Engineering, Huazhong University of Science and Technology, Wuhan, China.

W. Meng is with the School of Information Engineering, Wuhan University of Technology, Wuhan, China, and also with the School of Electronic and Electrical Engineering, University of Leeds, Leeds, UK.

S. Xie is with the School of Electronic and Electrical Engineering, University of Leeds, Leeds, UK, and also with the College of Electromechanical Engineering, Qingdao University of Science and Technology, Qingdao, China.

Up to now, many efforts have been devoted to the tracking design of mobile robots [6]-[8]. Note that most existing controllers are implemented on the explicit knowledge of the robotic dynamic models. However, formulating an accurate dynamic model has to encounter the high coupling problems between the mobile platform and its mounted robot arms. Moreover, the dynamic model-based controller may not work well due to the existence of disturbances and nonholonomic constraints, which may lead to either bad performance or unstable system behavior. To overcome these limitations, sliding mode control (SMC) guarantees asymptotic stability and strengthens robustness in the presence of strong nonlinearity and uncertainty [9], [10]. There have been some cases of SMC for mobile robot applications. For example, integrating extended state observe, Chao et al. present an SMC for a three-wheeled omnidirectional mobile robot with enhanced computation cost [11]; in [12], an SMC technique combined with neural network is developed for an OMR to coordinately follow the desired trajectory effectively.

Although SMC provides a good way for tracking control of an OMR, there are still some insufficiencies need to be further considered: a) The majority of SMC designs are implemented in the dynamic control framework, and the torque vibrations and wheel/ground interactions cannot be ignored for a dynamic controller [13]. By allocating the kinematic SMC, the OMR is able to retain the control simplicity and accuracy simultaneously. However, it is not easy to construct such a chattering-free SMC design due to the coupling of kinematic robotic states. It is well-known that the offset model of an OMR is expressed by the angle component and X-Y axes components. Thus, the standard sliding surfaces that completely decouple the system states are inapplicable since the dimension of the OMR outputs is three (i.e., three degree-of-freedom in the longitudinal, lateral and angular directions), but that of the sliding mode determined by the inputs is two (i.e., driving and steering velocities). b) The existing SMC solutions only concern a mobile robot with only single-mode, but multiple available modes of the OMR should be considered. Benefiting from regulating the configurated modes adaptively, the robotic controller is capable of improving the convergence of the state errors and system robustness. Unfortunately, the application of mode-switched controllers based on SMCs for such an OMR seems to be absent in the existing literature, which motivates us to contribute in this paper.

Consequently, we propose a switching-based coupled SMC (CSMC) method for precise trajectory tracking of a developed OMR. The key contributions of this paper are summarized as follows: 1) A general state error model is constructed to denote the available multiple modes of the OMR uniformly. 2) A new coupled sliding surface vector is presented to guarantee that the tracking error converges to zero, and a novel modified

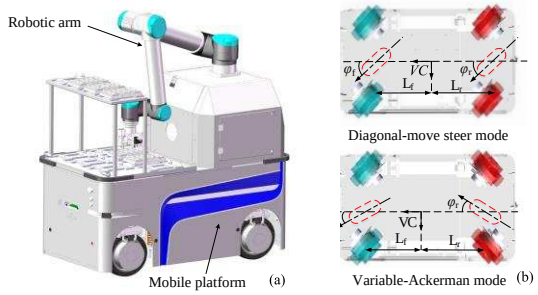

Fig. 1 The developed OMR. (a) prototype; (b) multiple modes.

reaching laws are proposed to eliminate the chattering phenomenon. 3) With a two-stage fuzzy logic system, the OMR achieves the optimal autonomous switched control by using the desired trajectory information and current state errors. 4) Under complex conditions, the experiments verify the effectiveness and practicability of this method.

The remainder is organized as follows: Section II describes the kinematic multiple modes of the developed OMR. The switched CSMC is given in Section III, followed by the stability analysis in Section IV. Experimental results and conclusions are provided in Section V and VI, respectively.

II. Multiple Kinematic Modes of the OMR

As illustrated in Fig. 1, with all-wheel-independently-steer technique, the OMR can achieve diversified steering modes, such as zero-radius mode, diagonal-move steer mode, variable-Ackerman mode. Consequently, this OMR has good driving mobility and maneuverability to adapt to different topographic environments. It should be mentioned that the zero-radius steer mode is used to avoid the robot position deviation or skid/slip by setting the left and right wheels in opposite directions to achieve pivot steer. For zero-radius turn, independent wheel-hub motors are adopted in our prototype to implement the yaw moment control and meanwhile regulate the tuning speed. The pivot steer movement of this mode is easy to realize, and it is omitted here due to the space limit. In diagonal-move steer mode, the front and rear wheels are steered to the same directions. Hence, the OMR can move diagonally or even laterally, which enables it to move from one point directly to another point without yaw motion. Therefore, good locomotion efficiency and accuracy can be expected. In variable-Ackerman mode, by adjusting the relationship between the front wheels and rear wheels, the OMR can change the steering radius and obtain high maneuverability to negotiate the environment with various operating demands. Specially, by steering the front wheel only, the OMR is worked in the conventional Ackerman mode that achieves high-speed steer; when controlling the front and rear wheels in opposite angles, the robot with double-axle steer mode reduces the steering radius and obtains a quick yaw response in a narrow space.

Moreover, the kinematic model of an OMR is simplified as a bi-steerable model with two virtual wheels which denote the front and rear axles, as shown in Fig. 1(b). Suppose that the OMR state is defined by $\mathbf{q}$, the robot position is (x, y), θ denotes the robot orientation and φ_f is the front steering angle. Then, we give the following kinematic models relating to the employed OMR modes.

a) Diagonal-move steer mode

$$\dot{\mathbf{q}} = [\dot{\mathrm{x}} \quad \dot{\mathrm{y}} \quad \dot{\varphi}_\mathrm{f}]^\mathrm{T} = \begin{bmatrix} \cos\varphi_\mathrm{f} & \sin\varphi_\mathrm{f} & 0 \\ 0 & 0 & 1 \end{bmatrix}^\mathrm{T} \begin{bmatrix} \mathrm{v} \\ \omega \end{bmatrix} \tag{1}$$

b) Variable-Ackerman steer mode

$$\dot{\mathbf{q}} = \begin{bmatrix} \dot{\mathrm{x}} \\ \dot{\mathrm{y}} \\ \dot{\theta} \end{bmatrix} = \begin{bmatrix} \cos\theta & \sin\theta & \dfrac{(\mathrm{k}_1+1)\tan\varphi_\mathrm{f}}{(\mathrm{k}_1+\mathrm{k}_2)\times \mathrm{L}} \\ 0 & 0 & 1 \end{bmatrix}^\mathrm{T} \begin{bmatrix} \mathrm{v} \\ \omega \end{bmatrix} \tag{2}$$

where v and ω denote the driving velocity and rotation rate of the robot main body, separately, $\mathrm{L} = \mathrm{L}_\mathrm{f} + \mathrm{L}_\mathrm{r}$ denotes the robot length, k_1 is the coefficient determined by the steering angles of the virtual front wheel φ_f and rear wheel φ_r, i.e., $\mathrm{k}_1 = \tan(\varphi_\mathrm{f}) / \tan(-\varphi_\mathrm{r})$, k_2 is a user-defined configuration parameter. Specifically, if $\mathrm{k}_1 = 0$ and $\mathrm{k}_2 = 1$, the robot is with commonly-used Ackerman mode while it is in double-axle steer mode when we adopt $\mathrm{k}_1 = 1$ and $\mathrm{k}_2 = 0$.

Remark 1 : It is noted that in diagonal-move steer mode, the θ remains constant during the whole operation, and thus it is an unnecessary kinematic state as depicted in (1). As for variable-Ackermann steer mode, if the steering rate upper limit is high enough, the steering angle φ_f can be instantaneously regulated using a lower-level controller [14]. In this sense, φ_f is considered as an internal articulation.

III. Switching-based CSMC Design

A. Unified State Error Model

For diagonal-move steer mode, defining a reference state vector $\mathbf{q}_\mathrm{r} = (\mathrm{x}_\mathrm{r}, \mathrm{y}_\mathrm{r}, \varphi_\mathrm{fr})^\mathrm{T}$ and a reference control signal vector $\mathbf{u}_\mathrm{r} = (\mathrm{v}_\mathrm{r}, \omega_\mathrm{r})^\mathrm{T}$, the derivative of $\mathbf{q}_\mathrm{r}$ is derived as

$$\dot{\mathbf{q}}_\mathrm{r} = \begin{bmatrix} \dot{\mathrm{x}}_\mathrm{r} \\ \dot{\mathrm{y}}_\mathrm{r} \\ \dot{\varphi}_\mathrm{fr} \end{bmatrix} = \begin{bmatrix} \mathrm{v}_\mathrm{r}\cos\varphi_\mathrm{fr} \\ \mathrm{v}_\mathrm{r}\sin\varphi_\mathrm{fr} \\ \omega_\mathrm{r} \end{bmatrix} = \begin{bmatrix} \cos\varphi_\mathrm{fr} & 0 \\ \sin\varphi_\mathrm{fr} & 0 \\ 0 & 1 \end{bmatrix} \mathbf{u}_\mathrm{r} \tag{3}$$

Then, the state error vector $\mathbf{q}_\mathrm{e}$ is determined by

$$\mathbf{q}_\mathrm{e} = \mathbf{q} - \mathbf{q}_\mathrm{r} = \begin{bmatrix} \mathrm{x}_\mathrm{e} \\ \mathrm{y}_\mathrm{e} \\ \varphi_\mathrm{fe} \end{bmatrix} = \begin{bmatrix} \cos\varphi_\mathrm{f} & \sin\varphi_\mathrm{f} & 0 \\ -\sin\varphi_\mathrm{f} & \cos\varphi_\mathrm{f} & 0 \\ 0 & 0 & 1 \end{bmatrix} \begin{bmatrix} \mathrm{x}_\mathrm{r} - \mathrm{x} \\ \mathrm{y}_\mathrm{r} - \mathrm{y} \\ \varphi_\mathrm{fr} - \varphi_\mathrm{f} \end{bmatrix} \tag{4}$$

Based on the kinematic state (1) and its error vector (4), one can construct the following kinematics

$$\begin{cases} \dot{\mathrm{x}}_\mathrm{e} = \omega \mathrm{y}_\mathrm{e} - \mathrm{v} + \mathrm{v}_\mathrm{r}\cos\varphi_\mathrm{fe} \\ \dot{\mathrm{y}}_\mathrm{e} = -\omega \mathrm{x}_\mathrm{e} + \mathrm{v}_\mathrm{r}\sin\varphi_\mathrm{fe} \\ \dot{\varphi}_\mathrm{fe} = \omega_\mathrm{r} - \omega \end{cases} \tag{5}$$

Relating to variable-Ackerman mode, we revise the control input vector as $[\mathrm{v}', \omega']$, where v' remaining as the robot forward speed and ω' is an intermediate variable determined by $\omega' = (\mathrm{k}_1+1)\tan\varphi_\mathrm{f} / (\mathrm{k}_1\mathrm{L} + \mathrm{k}_2\mathrm{L}) + \omega$. Therefore, we may get the simplified kinematics

$$\dot{\mathbf{q}} = \begin{bmatrix} \dot{\mathrm{x}} \\ \dot{\mathrm{y}} \\ \dot{\theta} \end{bmatrix} = \begin{bmatrix} \cos\theta & 0 \\ \sin\theta & 0 \\ 0 & 1 \end{bmatrix} \begin{bmatrix} \mathrm{v}' \\ \omega' \end{bmatrix} \tag{6}$$

Likewise, with a reference state vector $\mathbf{q}_\mathrm{r} = (\mathrm{x}_\mathrm{r}, \mathrm{y}_\mathrm{r}, \theta_\mathrm{r})^\mathrm{T}$, the corresponding kinematic error vector $\mathbf{q}_\mathrm{e}$ is given by

$$\mathbf{q}_e = \begin{bmatrix} x_e \\ y_e \\ \theta_e \end{bmatrix} = \begin{bmatrix} \cos\theta & \sin\theta & 0 \\ -\sin\theta & \cos\theta & 0 \\ 0 & 0 & 1 \end{bmatrix} \begin{bmatrix} x_r - x \\ y_r - y \\ \theta_r - \theta \end{bmatrix} \tag{7}$$

Define the reference control vector as $\mathbf{u}_r' = (v_r', \omega_r')^T$. The combination of $\mathbf{u}_r'$ and (7) yields the state error kinematics

$$\begin{cases} \dot{x}_e = \omega' y_e - v' + v_r' \cos\theta_e \\ \dot{y}_e = -\omega' x_e + v_r' \sin\theta_e \\ \dot{\theta}_e = \omega_r' - \omega' \end{cases} \tag{8}$$

To formulate the unified state error model, we construct a variable z with it being $z = \varphi_f$ in diagonal-move steer mode while $z = \theta$ in variable-Ackerman mode. Finally, we can obtain the following unified state model for the OMR with multi-modes

$$\begin{cases} \dot{x}_e = \omega_z y_e - v_z + v_{zr} \cos z_e \\ \dot{y}_e = -\omega_z x_e + v_{zr} \sin z_e \\ \dot{z}_e = \omega_{zr} - \omega_z \end{cases} \tag{9}$$

where ω_z, v_z, v_{zr} and ω_{zr} are the corresponding unified variables that can be derived from (5) and (8).

B. CSMC Control Law

For diagonal-move steer mode and variable-Ackerman steer mode, trajectory-tracking involves three state errors, i.e., (x_e, y_e, z_e) and only two control inputs. This implies that the traditional decoupled SMC solutions are impractical for such an OMR application. Inspired by [15], [16], we provide the following new coupled sliding surface vector $\mathbf{S}$

$$\begin{aligned} \mathbf{S} &= [s_1 \quad s_2]^T \\ &= \begin{bmatrix} \dot{x}_e + x_e \\ \dot{y}_e + y_e - \dot{x}_e - x_e + \text{sign}(y_e - \dot{x}_e - x_e)|z_e| \end{bmatrix} \end{aligned} \tag{10}$$

where $\text{sign}(*)$ denotes the sign function.

To design a stable CSMC, the control law should satisfy the sliding condition and reaching condition. The derivatives of the sliding surfaces are calculated using

$$\dot{s}_1 = \ddot{x}_e + \dot{x}_e \tag{11}$$

$$\dot{s}_2 = \ddot{y}_e + \dot{y}_e - \ddot{x}_e - \dot{x}_e + \text{sign}(y_e - \dot{x}_e - x_e)(d\,|\,z_e\,|/dt) \tag{12}$$

Substituting the errors from (9) into (11) and (12) yields

$$\dot{s}_1 = \omega_z y_e - v_z + v_{zr} \cos z_e + \ddot{x}_e \tag{13}$$

$$\begin{aligned} \dot{s}_2 = {} & \dot{v}_{zr} \sin z_e + \dot{z}_e v_{zr} \cos z_e - \dot{\omega}_z x_e - \omega_z \dot{x}_e \\ & - \ddot{x}_e - \dot{x}_e + \text{sign}(y_e - \dot{x}_e - x_e)(d\,|\,z_e\,|/dt) + \dot{y}_e \end{aligned} \tag{14}$$

Assuming that the OMR system is in the sliding surfaces, i.e., $\dot{s}_1 = \dot{s}_2 = 0$, the sliding laws v_{slide} and ω_{slide} can be obtained by utilizing the invariance principle

$$v_{slide} = \frac{1}{\cos z_e}(v_z - \ddot{x}_e - \omega_z y_e) \tag{15}$$

$$\omega_{slide} = \frac{\dot{\omega}_z x_e + \omega_z \dot{x}_e + \ddot{x}_e + \dot{x}_e - y_e - \dot{v}_{zr} \sin z_e}{v_{zr} \cos z_e + \text{sign}(y_e - \dot{x}_e - x_e)\text{sign}(z_e)} + \omega_z \tag{16}$$

With suitable reaching laws, which drive the state errors on the sliding surface asymptotically, that can help to diminish the inescapable chattering. We subsequently design v_{reach} and v_{reach} for linear and angular velocities as

$$v_{reach} = -p_1 s_1 - q_1 |s_1|^{\alpha_1} \tanh(s_1) \tag{17}$$

$$\omega_{reach} = -p_2 s_2 - q_2 |s_2|^{\alpha_2} \tanh(s_2) \tag{18}$$

where $p_{i=1,2} \in (0,\infty)$, $q_{i=1,2} \in (0,\infty)$ and $\alpha_{i=1,2} \in [0,1]$ are the coefficients used to specify different rates for the sliding surfaces and yields different structures in the reaching phase.

Integrating of (9) and (15)-(18) results in the control laws expressed as below

$$v_c = \frac{-p_1 s_1 - q_1 |s_1|^{\alpha_1} \tanh(s_1)}{\cos z_e} + v_{slide} \tag{19}$$

$$\omega_c = \frac{-p_2 s_2 - q_2 |s_2|^{\alpha_2} \tanh(s_2)}{v_{zr} \cos z_e + \text{sign}(y_e - \dot{x}_e - x_e)\text{sign}(z_e)} + \omega_{slide} \tag{20}$$

Remark 2 : In conventional SMC, the discontinuous term $\text{sign}(*)$ is applied to the reaching law due to imprecision of system modeling and disturbances. However, it leads to an undesired chattering phenomenon, which may impose a vibration or perturbation on the system responses. In this paper, we employ the $\tanh(*)$ function to offer a smooth switching of sliding mode to tackle the chattering effectively. Meanwhile, we add proportional rate terms $-p_1 s_1$ and $-p_2 s_2$ to force the state to approach the sliding surface faster when the state is far away from the switching manifold, and we use the power rate terms to reduce the reaching speed when the state is near the manifold. Hence, the tradeoff between the reaching time and level of chattering can be balanced.

Remark 3 : As studied in [17], the traditional constant proportional rate reaching law has a fast response however the reaching law is not adjustable; the demerit feature of the power rate reaching law is the deduction of its robustness due to the rapid lessening of the exponential term. The adopted reaching laws (17) and (18) bring advantages such as gain adaption regarding the sliding surface, smaller reaching time and chattering reduction.

Remark 4 : Practically, the magnitude and rate of the CSMC reaching laws can be regulated online whilst guaranteeing a sliding motion. The main interest is to handle the uncertainties and perturbation effects, thereby producing lower chattering. The adaptive SMC has been proposed and has been evaluated as an effect way for tracking control. In this sense, we can generate fuzzy logic system or neural network rules using the tracking error to enhance the tracking robustness of the developed OMR system [14].

D. Modes Switching Mechanism

In industrial scenarios, the developed OMR will have various desired and actual outputs, errors, as well as the control input signals, especially when performing in a confined space or uneven environment. As the OMR has multiple available modes, it is difficult to be certain of the operational mode using analytic methods. To address the above challenge, by regarding each alternative mode as a subsystem, we employ the information of current state and desired path to make the selection of optimal mode agnostic and meaningful across different requirements and situations.

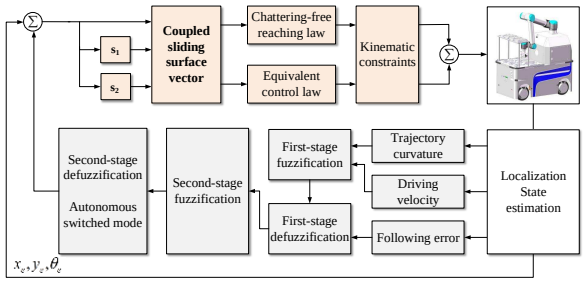

Fig. 2 The switching-based CSMC framework

To this end, a two-stage fuzzy switching technique is proposed to achieve an autonomous switched OMR. The basis of this adaptive technique is to obtain the definitive operational mode utilizing the weighted average of regulation rules. Each stage of the fuzzy system adopts a fuzzification process that maps the crisp value of inputs to linguistic variables using membership functions. Here, the inputs to the fuzzification process of the first stage are the curvature of the desired trajectory and driving velocity. Associating with the following error, the output of the first-stage serves as the input of next stage, which generates a supervisory variable to determine the most suitable mode for the present cycle time. Specifically, the triangular membership functions are considered for fuzzy mapping and five linguistic variables are considered for each input variable of the constructed two-stage, i.e., very small (VS), small (S), medium (M), big (B), very big (VB), whereas the output variable is represented in five linguistic values such as zero error (ZE), positive small (PS), positive medium (PM), positive big (PB), positive large (PL). Then, the aggregate fuzzy output sets for the defuzzification process is converted to precise variables, which is determined by the singleton fuzzifier and center average defuzzifier [18]. In this way, we can obtain an autonomous switched robust controller.

IV. Stability Analysis

Theorem 1: With the proposed sliding surfaces (10) and control laws determined by (19) and (20), the finite time reachability of CSMC is guaranteed. Moreover, the derived optimal solution stabilizes the resulted OMR system.

Proof: Let us consider a Lyapunov candidate $V = 0.5\mathbf{S}^2$. The derivative of V is given as below

$$\begin{aligned}\dot{V} &= s_1 \cdot \dot{s}_1 + s_2 \cdot \dot{s}_2 = s_1 \cdot (\ddot{x}_e + \dot{x}_e) + \\ & s_2 \cdot \left(\ddot{y}_e + \dot{y}_e - \ddot{x}_e - \dot{x}_e + \text{sign}(y_e - \dot{x}_e - x_e)(d\,|\,z_e\,|/dt) \right)\end{aligned} \tag{21}$$

By combining (9) and (21), one can obtain that

$$\begin{aligned}\dot{V} &= s_1 \cdot (\ddot{x}_e + \omega_z y_e - v_z + v_c \cos z_e) \\ &+ s_2 \cdot (\dot{v}_{zr} \sin z_e + (\omega_c - \omega_z) v_{zr} \cos z_e - \dot{\omega}_z x_e - \omega_z \dot{x}_e \\ &- \ddot{x}_e - \dot{x}_e + \text{sign}(y_e - \dot{x}_e - x_e)\text{sign}(z_e)(\omega_c - \omega_z) + \dot{y}_e)\end{aligned} \tag{22}$$

Adding the presented laws (19), (20) into (22) results in

$$\begin{aligned}\dot{V} &= s_1 \cdot \left(-p_1 s_1 - q_1 |s_1|^{\alpha_1} \tanh(s_1) \right) \\ &+ s_2 \cdot \left(-p_2 s_2 - q_2 |s_2|^{\alpha_2} \tanh(s_2) \right) \\ &= -p_1 s_1^2 - q_1 |s_1|^{\alpha_1} s_1 \tanh(s_1) - p_2 s_2^2 - q_2 |s_2|^{\alpha_2} s_2 \tanh(s_2)\end{aligned} \tag{23}$$

From (23), $\dot{V} < 0$ holds for $q_{i=1,2}$ and $p_{i=1,2}$ being positive definite. Then, it is concluded that the resulted OMR system is stable with the proposed control laws (19) and (20). For the applied chattering-free reaching law (17), if the initial state $s_1(t_0^{s_1})$ satisfies $s_1(t_0^{s_1}) \geq 0$, with the assumption that $\tanh(s_1) \simeq \beta_1$ where $\beta_1 \in [0,1]$, we get the integration of (17) between $t_0^{s_1}$ and the reaching time $t_{reach}^{s_1}$ as follows

$$\int_{s_1(t_0^{s_1}=0)}^{s_1(t_{reach}^{s_1})} \frac{ds_1}{p_1 s_1 + q_1 |s_1|^{\alpha_1} \beta_1} = \int_{t_0^{s_1}=0}^{t_{reach}^{s_1}} -dt \tag{24}$$

Since $s_1(t_{reach}^{s_1}) = 0$, the reaching time is determined by

$$t_{reach}^{s_1} = \frac{1}{p_1(1-\alpha_1)} \ln\left(\frac{p_1 s_1(t_0^{s_1})^{1-\alpha_1} + q_1 \beta_1}{q_1 \beta_1} \right) \tag{25}$$

On the other hand, if the initial state of switching manifold meets $s_1(t_0^{s_1} = 0) < 0$ and the following condition is satisfied

$$t_{reach}^{s_1} = \frac{1}{p_1(1-\alpha_1)} \ln\left(\frac{p_1 |s_1(t_0^{s_1})|^{1-\alpha_1} + q_1 \beta_1}{q_1 \beta_1} \right) \tag{26}$$

the OMR system will converge to the switching manifold in finite time. Likewise, as for s_2, we can derive the corresponding reaching time $t_{reach}^{s_2}$ that of the same structure with $t_{reach}^{s_1}$. In conclusion, if the following inequalities hold

$$t \geq \max\left\{ t_{reach}^{s_1}, t_{reach}^{s_2} \right\} \tag{27}$$

the OMR system will slide to switching manifold at any initial state in finite time. Here completes the proof. □

Theorem 2: When the reaching conditions are satisfied, the presented CSMC ensures the asymptotical convergence of state error vector (9) .

Proof: Arriving at the switching manifold, we can obtain $\mathbf{S} = \mathbf{0}$, i.e.,

$$s_1 = \dot{x}_e + x_e = 0 \tag{28}$$

$$s_2 = \dot{y}_e + y_e - \dot{x}_e - x_e + \text{sign}(y_e - \dot{x}_e - x_e)|z_e| = 0 \tag{29}$$

It can be known that if s_1 converges to zero, trivially x_e converges to zero. Substituting (28) into (29), we get

$$s_2 = \dot{y}_e + y_e + \text{sign}(y_e)|z_e| = 0 \tag{30}$$

By (30), since $|z_e|$ is always bounded, we can obtain the following inequalities regarding $\dot{y}_e$ and y_e

$$y_e > 0 \Rightarrow \dot{y}_e < 0 \tag{31}$$

$$y_e < 0 \Rightarrow \dot{y}_e > 0 \tag{32}$$

Hence, the equilibrium state of y_e is asymptotically stable. Finally, it is concluded from $s_2 = 0$ that the convergence of y_e and $\dot{y}_e$ leads to convergence of $|z_e|$ to zero. Here completes the proof. □

V. Experimental Validation

Experiments on a commercialized OMR are carried out in this section to verify the validity of the switched CSMC. The developed four-wheel-steerable four-wheel-driven mobile robot called FORALLBOT is shown in Fig. 3, which has high maneuverability and flexibility in an uneven floor or confined spaces. Each wheel has two degree of freedom to move actively in the orientation of wheels' heading and rotation

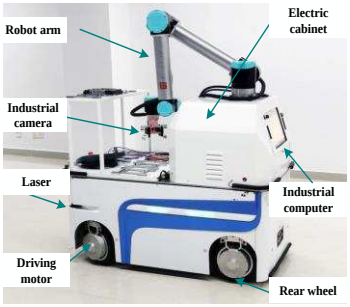

Fig. 3 The experimental platform

and rotation. This OMR has some prominent features, such as automatic charging, anti-crash measures, trackless autonomous navigation and vision-based operating the workpiece. To achieve autonomous navigation, the main components of this OMR include robot arm, electric cabinet, industrial camera, laser and driving motors. The hardware architecture of the OMR system is typically constituted by the modules of perception, decision making and movement control. The four wheels of the robot are driven by hub motors (rated torque 0.95 Nm, rated current 10 A, 2500 pulses/turn). The proposed CSMC method is implemented using C/C++ code and standard programming techniques in an embedded PC with a specification of 2.59 GHz and 8G RAM.

For implementation, the related parameters of CSMC method are specified as: $L_f = L_r = 0.445$ m, $k_1 = 0$, $k_2 = 1$, $p_1 = 1.25$, $p_2 = 4.75$, $q_1 = 1.2$ and $q_2 = 2.3$. In the experiment, we consider the traditional proportion integration (PI) controller under diagonal mode, CSMC-based Ackerman mode, CSMC-based diagonal mode for comparison. It is noted the parameters of PI controller are set as 1.8 and 0.75 for the proportional gain and integral gain, respectively.

As depicted in Fig. 4, the desired trajectory can be divided into two stages, i.e., smooth-turning stage and point-to-point move mode. It should be mentioned that the reference orientation of the OMR keeps the same with the last moment of the sharp tuning. The initial poses of the OMR are assumed to be [0 0.5 m –0.5 rad]. The corresponding errors are presented in Fig. 5-Fig. 7. The results show that the trajectory of the OMR is successfully tracked with the proposed switched motion controller. For the situation that uses PI controller and diagonal mode, there is always a notable overshoot/undershoot in all the tracking errors with maximum magnitude of 0.15 m, 0.5 m and 0.62 rad associating to x_e, y_e and θ_e, respectively. Resulting from steering only the front wheel, we can achieve better performance in the smooth-tuning stage with Ackerman mode, which regulates the robot orientation in high-speed and achieves relative-low θ_e, as shown in Fig. 7. In comparison, diagonal mode behaves better in the point-to-point stage due to its good locomotion characteristics. By switching the modes adaptively, the OMR system is capable of improving the tracking efficiency and accuracy. Moreover, we adopt the L2 norm tracking error determined by $(x_e^2 + y_e^2 + \theta_e^2)^{1/2}$ to evaluate the tracking performance shown in Fig. 8. The figures verify that the proposed method is able to achieve comprehensive tracking performance.

For the designed coupled sliding surfaces, the vibration tendencies are denoted in Fig. 9. It is obvious that the sliding

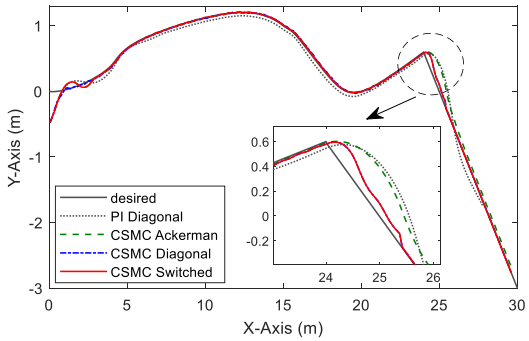

Fig. 4 The trajectory tracking responses

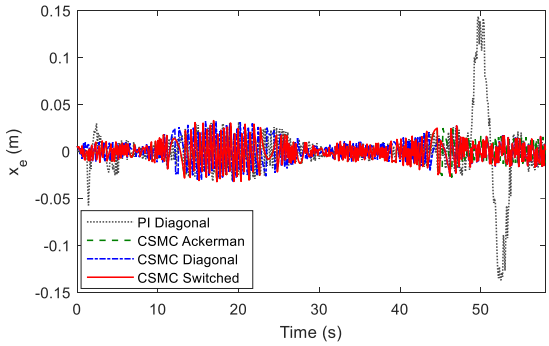

Fig. 5 The tracking error x_e

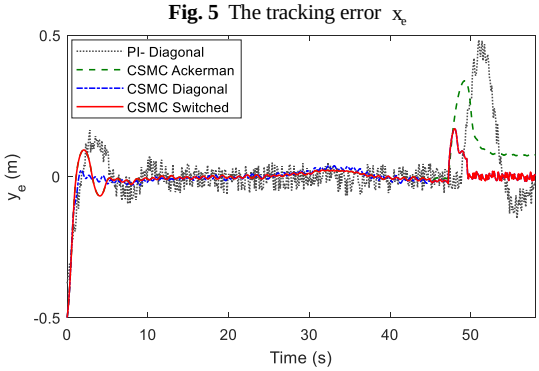

Fig. 6 The tracking error y_e

surfaces approach zero under the CSMC scheme, and some chattering can be found during the sharp tuning of the desired trajectory. With the switched method, we may mitigate the magnitudes of sliding motions to achieve an acceptable level quickly. Thus, the resulted OMR system can obtain satisfactory tracking performance.

To be more succinct, we have listed the performance indexes of the tracking errors with respect to the root mean square (RMS) and standard deviation (SD), as shown in TABLE 1. Compared with the traditional PI controller or the CSMC-based single-mode control system, the tracking errors can be significantly reduced by the proposed switched CSMC controller. Under our method, x_e and y_e of the single diagonal-move steer mode are enhanced by 84.8948% and 79.5782 % in terms of RMS. However, due to the kinematic constraints, θ_e of the single diagonal mode is the worst among the comparison modes. By using Ackerman mode in the first stage and switching to diagonal-move steer mode in the point-to-point stage, the RMS of θ_e can be decreased by 67.4350%. Therefore, the proposed controller is useful for the stabilization and error mitigation of the developed OMR system, which demonstrates the advantages of the proposed switched CSMC-based control method.

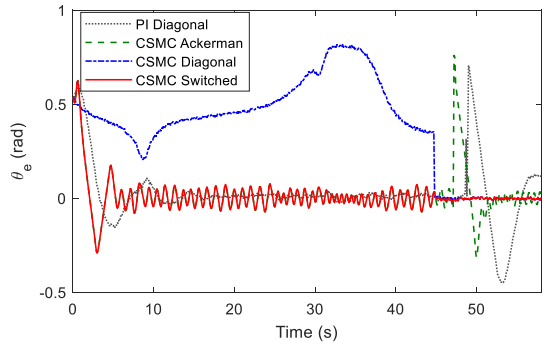

Fig. 7 The tracking error θ_e

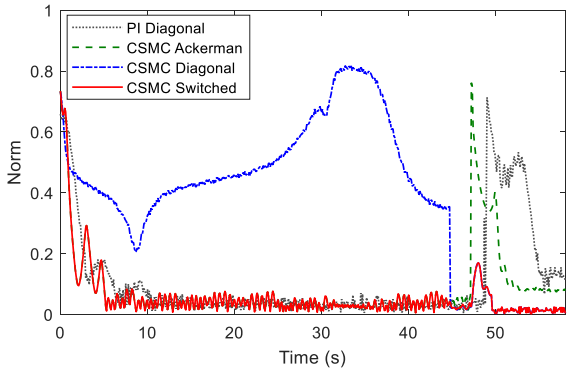

Fig. 8 The constructed norm of the errors

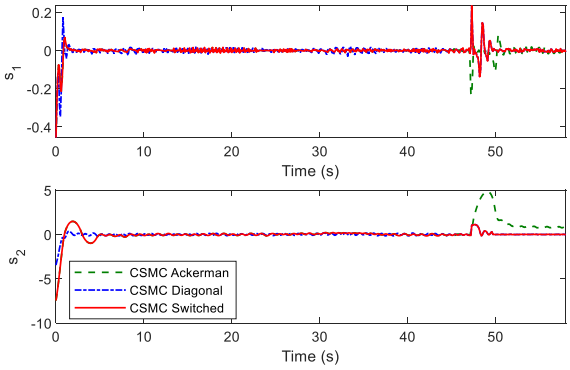

Fig. 9 The presented coupled sliding surfaces

TEBLE 1. PERFORMANCE INDEXES OF THE COMPARISON CONTROL SYSTEMS

Error	Index	PI Diagonal	CSMC Ackerman	CSMC Diagonal	CSMC Switched
x_e	RMS	0.0523	0.0078	0.0079	0.0076
	SD	0.0300	0.0116	0.0116	0.0114
y_e	RMS	0.6924	0.3856	0.1414	0.1491
	SD	0.1089	0.0806	0.0514	0.0528
θ_e	RMS	1.4924	0.9073	11.9954	0.4860
	SD	0.1594	0.1249	0.2467	0.0925

VI. CONCLUSION

This paper investigated the tracking control of an OMR with variable modes. A unified state error model was constructed to accommodate the optional kinematics configurations. Then, a novel CSMC scheme was proposed with a coupled sliding surface vector and modified reaching law so that the obtained system has smaller reaching time and chattering reduction. Based on the current state information and the curvature of the desired trajectories and driving velocity, autonomous switched robust controller is achieved by using a two-stage fuzzy logic system. Experimental results are exhibited to verify the effectiveness of the presented control strategy. The excellent properties of the proposed CSMC method with designed switched rules compared to the PI or CSMC with only one single-mode include better ability of robust path-following, tracking error alleviation and chattering-free switching.

REFERENCES

[1] X. Ding, Y. Liu, J. Hou, and Q. Ma, "Online Dynamic Tip-Over Avoidance for a Wheeled Mobile Manipulator With an Improved Tip-Over Moment Stability Criterion," IEEE Access, vol. 7, pp. 67632-67645, 2019.

[2] F. Chen, M. Selvaggio, and D. G. Caldwell, "Dexterous Grasping by Manipulability Selection for Mobile Manipulator with Visual Guidance," IEEE Trans. Ind. Inf., vol. 15, no. 2, pp. 1202-1210, Feb. 2019.

[3] J. Huang, T. Van Hung, and M. Tseng, "Smooth Switching Robust Adaptive Control for Omnidirectional Mobile Robots," IEEE Trans. Control Syst. Techno., vol. 23, no. 5, pp. 1986-1993, Sept. 2015.

[4] L. Xiao, et al., "Design and Analysis of FTZNN Applied to the Real-Time Solution of a Nonstationary Lyapunov Equation and Tracking Control of a Wheeled Mobile Manipulator," IEEE Trans. Ind. Inf., vol. 14, no. 1, pp. 98-105, Jan. 2018.

[5] J. Ni, J. Hu, and C. Xiang, "Robust Control in Diagonal-move Steer Mode and Experiment on an X-by-Wire UGV," IEEE/ASME Trans. Mechatron., vol. 24, no. 2, pp. 572-584, April 2019.

[6] G. D. White, R. M. Bhatt, C. P. Tang, and V. N. Krovi, "Experimental Evaluation of Dynamic Redundancy Resolution in a Nonholonomic Wheeled Mobile Manipulator," IEEE/ASME Trans. Mechatron., vol. 14, no. 3, pp. 349-357, June 2009.

[7] Y. Chen, Z. Li, H. Kong, and F. Ke, "Model Predictive Tracking Control of Nonholonomic Mobile Robots With Coupled Input Constraints and Unknown Dynamics," IEEE Trans. Ind. Inf., vol. 15, no. 6, pp. 3196-3205, June 2019.

[8] G. B. Avanzini, A. M. Zanchettin, and P. Rocco, "Constrained model predictive control for mobile robotic manipulators," Robotica, vol. 36, no. 1, pp. 19-38, 2018.

[9] N. Chen N, et al., "An adaptive sliding mode backstepping control for the mobile manipulator with nonholonomic constraint," Commun. Nonlinear Sci. Num. Simu., vol. 18, no. 10, pp. 2885-2899, 2013.

[10] I. S. Se and S. I. Han, "Dual closed-loop sliding mode control for a decoupled three-link wheeled mobile manipulator," ISA Trans., vol. 80, pp. 322-335, 2018.

[11] C. Ren, X. Li, X. Yang, and S. Ma, "Extended State Observer-Based Sliding Mode Control of an Omnidirectional Mobile Robot With Friction Compensation," IEEE Trans. Ind. Electron., vol. 66, no. 12, pp. 9480-9489, Dec. 2019.

[12] D. Xu, D. Zhao, J. Yi, and X. Tan, "Trajectory Tracking Control of Omnidirectional Wheeled Mobile Manipulators: Robust Neural Network-Based Sliding Mode Approach," IEEE Trans. Syst., Man, Cybern., Part B (Cybern.), vol. 39, no. 3, pp. 788-799, June 2009.

[13] R. Solea and U. Nunes, "Trajectory planning and sliding-mode control based trajectory-tracking for cybercars," Integrated Computer-Aided Eng., vol. 14, no. 1, pp. 33-47, 2007.

[14] B. Paden, M. Čáp, S. Z. Yong, D. Yershov, and E. Frazzoli, "A Survey of Motion Planning and Control Techniques for Self-Driving Urban Vehicles," IEEE Trans. Int. Veh., vol. 1, no. 1, pp. 33-55, March 2016.

[15] J. Yang and J. Kim J, "Sliding mode control for trajectory tracking of nonholonomic wheeled mobile robots," IEEE Trans Robotics Autom. vol. 15, no. 3, pp. 578-87, 1999.

[16] Y. Kanayama, Y. Kimura, F. Miyazaki, and T. Noguchi, "A stable tracking control method for an autonomous mobile robot," In Proc., IEEE Int. Conf. Robotics Autom., Cincinnati, USA, pp. 384-389, 1990.

[17] S. M. Mozayan, M. Saad, H. Vahedi, H. Fortin-Blanchette, and M. Soltani, "Sliding Mode Control of PMSG Wind Turbine Based on Enhanced Exponential Reaching Law," IEEE Trans. Ind. Electron., vol. 63, no. 10, pp. 6148-6159, Oct. 2016.

[18] F. Wang and X. Zhang, "Adaptive Finite Time Control of Nonlinear Systems Under Time-Varying Actuator Failures," IEEE Trans. Syst., Man, Cybern.: Syst., vol. 49, no. 9, Sep. 2019.